MODEL R.F. CAVITY FOR N.I.N.A.

by

M. H. R. Donald

E. A. Hughes.

Daresbury Nuclear Physics Laboratory,
Daresbury,
Nr. Warrington,
Lancs.

APRIL 1964.

MODEL CAVITY R.F. FOR N.I.N.A.

APRIL 1964.

The accelerating structure for N.I.N.A. will consist of a resonant ring system of waveguide feeding five cavities, the whole system being tuned to a frequency of 407.88 mc/s. A diagram of the system is shown in Fig 1. The cavities will be of a triple-cell type and will be tuned in the π - mode. The parameters of the ring system demand that the Q external of the cavities shall be capable of being made of the order of 7000 when a 10 micro-amp beam is being accelerated. Also, since the signal which is applied to the cavity is being modulated, it is essential that the frequency splitting between the π - mode and the adjacent 0 - mode should give sufficient bandwidth so that the modulation will not excite the "0"-mode. The calculations on which the cavity design is based involve some degree of approximation and the purpose of the full size model cavity was to check that the design did in fact meet these criteria and that such a cavity had a sufficiently high shunt resistance to accelerate electrons to the required energy with the available power.

DESIGN OF CAVITY

The cavity is shown in Fig 2. The cells of the cavity are coupled together by round holes in the partitions between them. The π - mode is the perturbed mode in this arrangement.

The π - mode frequency ω_π is found from the 0 - mode frequency ω_0 by

$$\omega_\pi = \omega_0(1 - \delta)$$

where δ is the intercell coupling factor.

δ is directly related to the radius a of the coupling holes by

$$\delta = \frac{4}{3} \frac{a^3}{V} (2 H_o^2(0) - A_{ox}^2(0))$$

where V is the volume of a single cell; $H_o(0)$ is magnetic field at the centre of the hole; $A_{ox}(0)$ is the x- component of magnetic vector potential at the centre of the hole; and where $\overrightarrow{Z}$ is the axis of the cavity.

The diameter of the hole is primarilly governed by the diameter of the electron beam and was eventually fixed at 5.9". The length of each cell was made equal to half a wave-length i.e. 14.468". The cell radius r was calculated as approximately r = 11.13" and then the mode splitting worked out. This was done by substituting in the formula for δ the appropriate expressions for H_o and A_{ox}.

$$\delta = \frac{4}{3} \frac{a^3}{\pi r^2 \ell} \left\{ 2 \left(\frac{J_1(x,o)}{J_1(x,a)} \right)^2 - \left(\frac{J_o(x,o)}{J_1(x,a)} \right)^2 \right\}$$

J_o, J_1 are Bessel Functions

From this δ = 0.03769

A correction must be made for the finite thickness of the intercell partitions. These make the coupling holes act like cut-off waveguide with an attenuation

$$\frac{E}{E_o} = \exp\left(-2\pi\frac{Z}{\lambda_c}\sqrt{1-\left(\frac{\lambda_o}{\lambda_c}\right)^2}\right)$$

The final figure for γ is thus 0.0125 which makes

$$\omega_\pi - \omega_o = 5.08 \text{ mc/s.}$$

Thus each cell should correspond to a simple E010 cavity with resonant frequency 402.80 mc/s. Its diameter D = 2r is given by

$$D = \frac{\lambda_o X_{01}}{\pi}$$

where X_{01} is the 1st root of $J_o(x) = 0$.
From this D = 22.426".

The input aperture to the cavity was simply made as large as possible with the intention of stopping it down with irises as necessary.

The tuners consisted of large plates able to be screwed in and out. Two each were provided in the outer cells and three in the centre cell to try and offset the effect of the input aperture The final design is shown in Fig 2.

INVESTIGATION OF CAVITY PROPERTIES.

Tuning of Cavity:

Some preliminary experiments were first performed to establish roughly the resonant frequencies in the 0 and π - modes. The modes were identified by comparing phase between matched probes inserted in the cavity.

An attempt was then made to tune the cavity in the π - mode at 407.88 mc/s. In fact it proved impossible to tune the cavity properly at 407.88 mc/s, since the perturbation of the input aperture made the range of the centre cell tuners inadequate. The best arrangement was found to be a slightly reduced frequency and a slightly reduced field in the centre cell.

Under these tuning conditions the frequency separation between the "0" and "π" - modes was found to be 3.95 mc/s.

Q of Cavity:

The model was fabricated by brazing and would thus be expected to have a lower Q than the final cavities which, it is hoped, will be electroformed.

Two methods were used to measure the Q of the cavity. These were:

a) Half power points by transmission to internal probes

b) Various V.S.W.R. methods.

The second method was used as a check on the accuracy of the first. Over a series of results taken specifically to determine possible errors in the method, less than 2% variation occurred.

All measurements on the cavity were carried out with the circuit arrangement shown in Fig. 3. This itself is a model of the feeder arm from the ring system to the cavity.

Initially, the measured value of Q varied wildly. This was traced to the fact that the window clamping flange (see Fig 4) was making intermittent contact with the waveguide and cavity. It was cured by clamping the flange down on a metal gasket at the point B, thus connecting it solidly to the cavity.

A considerable number of Q measurements were made with various iris sizes and window thicknesses, at critical and maximum coupling. The coupling was varied, for any particular input aperture, by altering the position ℓ of the variable short circuit. The coupling was measured by a waveguide slotted line. Simultaneously a perturbation experiment was carried out as described in the next section to study cavity fields.

The Q measured directly is the loaded Q, Q_L. This is related to the unloaded Q, Q_o and the external Q, Q_{ext} by the equations:-

$$Q_o = Q_L (1 + \beta)$$

$$Q_o = \beta Q_{ext}$$

where β is the coupling factor, which is the V.S.W.R. measured with the slotted line.

$\beta > 1$ for overcoupled case.

$\beta < 1$ for undercoupled case.

Graphs 1, 2 and 3 show the variation of these parameters and a representative set of measurement are given in table 1.

It was found that if the short circuit was put at $l = 74.7$ cm $\pm \frac{3\lambda_g}{4}$ then maximum coupling was effected for all window configurations. It was also found that this length is not very critical.

CAVITY FIELDS & SHUNT RESISTANCE

The cavity fields were studied by passing a perturbing metal bead down the axis, Z, of the cavity. This shifts the resonant frequency by an amount of δf given by

$$\frac{\delta f}{f_o} = \frac{\pi a^3 \left(\frac{\mu H^2}{2} - \varepsilon E^2 \right)}{U}$$

Where:- a is the radius of the bead.

U is the stored energy in the cavity

ε is the permittivity.

H is assumed to be zero on the axis, so the perturbation δf caused by the bead at any point is a measure of the electric field strength at that point. Graphs 4 and 5 are plots of $\sqrt{\delta f}$ against bead position Z.

Notes The cavity axis, for the purpose of these measurements, was divided into arbitrary units 3.5 cm long for practical reasons. The diameter of the bead was 0.95 cm. The maximum frequency perturbation observed were of the order of 3 kc/s in 408 mc/s. The perturbed frequencies could be measured

to $\pm$ 5 c/s, but the accuracy of the experiment was reduced by thermal drift of the cavity.

The graphs show that the field distribution down the axis of the cavity is approximately sinusoidal. It will be noticed however, that there are some harmonics present, these being shown by the flattening of the curves round their maxima. For correct tuning, only odd harmonics were present, but when the field in the centre cell is different from that in the outer two cells a subharmonic at 3 times the wavelength of the fundamental was present.

These curves can be used to calculate the shunt resistance of the cavity. The shunt impedance of a resonant cavity used in a standing wave accelerator structure is defined (by analogy with the equivalent circuit) as

$$R_s = \frac{V_c^2}{2P}$$

where P is the power dissipated in the cavity and V_c is the accelerating voltage across the cavity, neglecting the transit time effect.

$$\text{Thus } V_c = \int_o^L E(z)\,dZ$$

where E is the axial electric field

L is the length of the cavity.

Q_o is defined as $\frac{\omega U}{P}$

$$\text{Thus } \frac{R_s}{Q_o} = \frac{1}{2\omega U}\left(\int_o^L E\,dZ\right)^2$$

$$\text{But } \frac{\pi a^3 \varepsilon E^2}{U} = \frac{\delta f}{f_o}$$

$$\text{so } \frac{R_s}{Q} = \frac{1}{2}\,\frac{1}{\omega \pi a^3 \varepsilon}\left(\int_o^L \sqrt{\frac{\delta f}{f_o}}\,dZ\right)^2$$

This formula takes account of the space harmonics but not the transit time.

The transit time factor will be $\frac{2}{\pi}$ for this cavity

Representative values of $\frac{R_s}{Q_o}$ calculated from these curves are:

1) No alumina window, 8" aperture.
$\frac{R_s}{Q_o} = 479 \pm 12$ ohms.

2) 9/16" Alumina Window, 8" aperature. $\frac{R_s}{Q_o} = 448 \pm 46$ ohms.

As a check for stray H-field on the axis of the cavity, due to the perturbation of the input window, an experiment was carried out with a P.T.F.E. bead which does not react to magnetic field. The perturbation due to a dielectric bead is less than that due to a metal bead in the same electric field by a factor of

$$\frac{k_e - 1}{k_e + 2}$$

where $k_e = \frac{\varepsilon}{\varepsilon_o}$

For P.T.F.E. this factor is very nearly $\frac{1}{4}$. For comparison two consecutive perturbation experiments were performed, first with a metal bead and then with a dielectric bead of the same diameter. The perturbations due to the P.T.F.E. bead were multiplied by 4 and plotted together with the metal bead graph for comparison in graph No. 6.

The value of $\frac{R_s}{Q_o}$ computed from the dielectric bead graph was

$$\frac{R_s}{Q_o} = .469 \text{ ohms.}$$

It can be seen from graph No 6 that there is negligible H-field present except in the region round the intercell coupling holes, where the field is small anyway.

The cavity was then tuned in the "0" - mode and a perturbation experiment was performed with a metal bead (note, since cavity was tuned for the "π" - mode the "0" - mode has very unequal fields in the 3 cells.) See graph No. 7.

The value of $\frac{R_s}{Q_o}$ from this graph is

$$\frac{R_s}{Q_o} = .565 \text{ ohms ("0" - mode).}$$

At the same time the Q of the cavity was measured for the maximum coupling condition when:-

$Q_u = 35,543$
$Q_L = 5,297$ } 0 - mode
$Q_{ext} = 6,224$
$\beta = 5.714$

EFFECTS OF END-PIPES:-

Bearing in mind that the final cavities will be connected to vacuum pipes and pumps, the cavity end pipes were extended by 6" to see if any field could be detected in the extensions. Graph No. 8 is a perturbation plot before and after the extensions were fitted.

Note. the actual values of the perturbations are not comparative since the tuning of the cavity was slightly altered at the same time.

It can be seen from the graph that electromagnetic field can be detected up to a distance approximately 4 cm. from the cavity. This minimum detectable field is about 2% of the peak cavity field.

RADIAL FIELD:-

An investigation of the radial field variations was carried out for the π- mode, by traversing a metallic bead across a central diameter of each cell. The differences between the central and outer cells will give an idea of the perturbation due to the waveguide to cavity coupling hole.

The bead was run through the gaps at the sides of the tuning plates. It's track is shown in Fig 5.

The results are shown on Graph No. 9. It can be seen from this that the point of maximum field is shifted slightly towards the input aperture in the centre cell.

LOADED CAVITY

The beam loading of the cavity was simulated by putting a graphite loaded thread down the axis of the cavity. This made the cavity, with 8" aperture and 9/16" thick window very nearly critically coupled when the moveable short circuit was at the position to give maximum coupling. The Q of the cavity was then measured and the axial field distribution was examined. The Q's are given below and the perturbations are plotted on graph No 10.

Cavity	Q_u	Q_L	Q_{ext}	β
Loaded	10,371	4182	7000	1.480
Unloaded	29,050	5512	6811	4.270

The value of Q_{ext} changes by less than 3% compared to a change of 64% in Q_u.

EQUIVALENT CIRCUIT OF CAVITY

An attempt was made to formulate an equivalent circuit for the cavity-short circuit system shown in Fig 3. The purpose of this circuit is to provide a rapid, fairly accurate method of calculating the behaviour of the system, with certain limitations, rather than to be a complete equivalent. It is required that the basic information needed to fix iris and window conditions is measured experimentally. All loss effects are neglected and only an ideal transformer is included in the circuit to give the coupling.

The parallel arrangement shown in Fig 6. was considered to be the most reasonable circuit and a preliminary experiment was performed to establish the position 1 of the variable short circuit with respect to its calibration scale. This was done by loading the cavity until it was critically coupled in the maximum coupling condition and varying the position of the short circuit until the admittance looking in at the centre line of the cavity input window was equivalent to a short circuit $\frac{\lambda_g}{2}$ away. Smith Chart No 1 is a plot of admittance for various positions of the short circuit with a diameter drawn through the equivalent short circuit position. The slight rotation of the admittance plot was attributed to the disturbed fields round the input window. This effect was included in the equivalent circuit by shifting the plane of the junction a distance d away from the physical

centre line of the input window. Similarly it was found that the length of the cavity arm was not exactly $\frac{\lambda g}{4}$, but was extended by a small distance d' depending on iris size. No simple way can be found of calculating these quantities and they will have to be measured for each set of conditions.

The information required to predict the behaviour of the system for any short circuit position l, is the measured value of β (the coupling factor) and the length d and d'. Since R_s is known this fixes the transformer turns ratio n in terms of Z_o by

$$n^2 = \frac{1}{\beta} \quad \frac{R_s}{Z_o}$$

The behaviour of the input admittance of the system can then be determined by summing the input admittances of the short circuit and cavity branch arms.

The equivalent circuit as thus formulated was tested by measuring the admittance of the system over a range of frequencies about the resonant frequency, for maximum and both critical coupling positions. Smith Charts 2 and 4 are plots of these admittances for 8" and 6" irises respectively. The behaviour under these conditions was then calculated and drawn out on Smith charts 3 and 5. Comparing 2 with 3 and 4 with 5 it can be seen that the predictions agree very well with experimental data, except that losses are neglected.

The variations in d and d' measured were:-

Iris Size	d cm.	d' cm.
8"	- 1.06	0.70
6"	- 0.635	0.92

CONCLUSIONS

Tuning:

It is impossible to tune the cavity properly with the centre cell at its present size. The diameter of the centre cell must therefore be reduced, by an amount calculated by proportion from the observed effect of the tuners to be 0.046"

Q_o, CAVITY FIELDS, $\frac{R_s}{Q_o}$: -

The measured value of Q_o at $\sim$ 30,000 was quite satisfactory and it was possible to get Q_{ext} to it's required value of $\sim$ 7,000.

The cavity fields showed little trace of stray H-field on the axis and the radial field in the centre cell was not seriously perturbed by the presence of the input aperture.

The measured value of $\frac{R_s}{Q_o}$ was satisfactory and since it is independent of cavity losses, it should be applicable to the final cavities. It should lead to shunt impedances of about 16.1 M.ohms (assuming Q_o of about 35,000).

END PIPES:-

Some field is detectable in the end pipes at short distances from the cavity and this should be born in mind when high power is used.

EQUIVALENT CIRCUIT:-

A satisfactory equivalent circuit has been formulated.

From this model a firm design has emerged for a prototype accelerating cavity, and firm figures are available for system design.

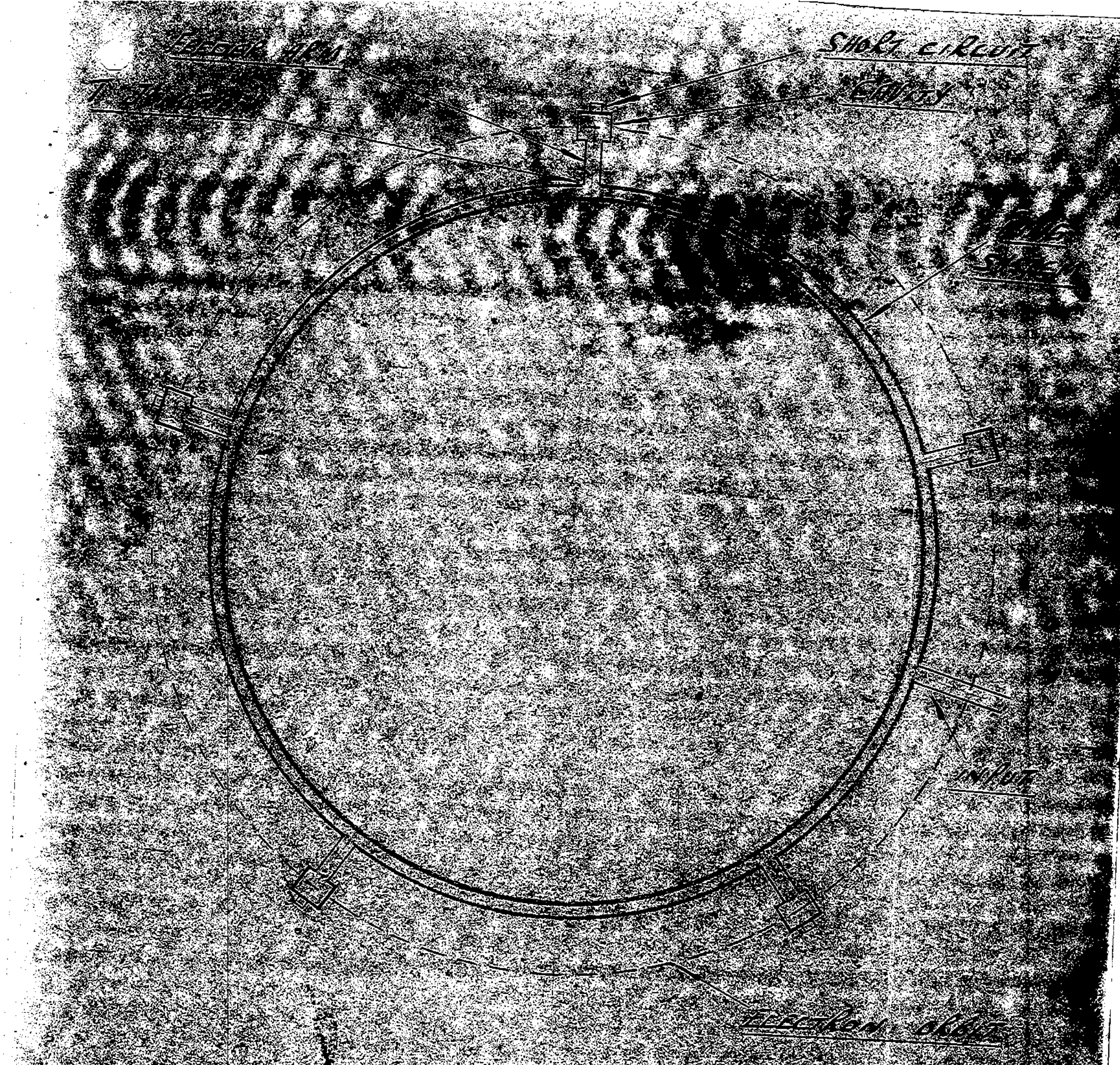

SCHEME OF RING SYSTEM FIG. 1.

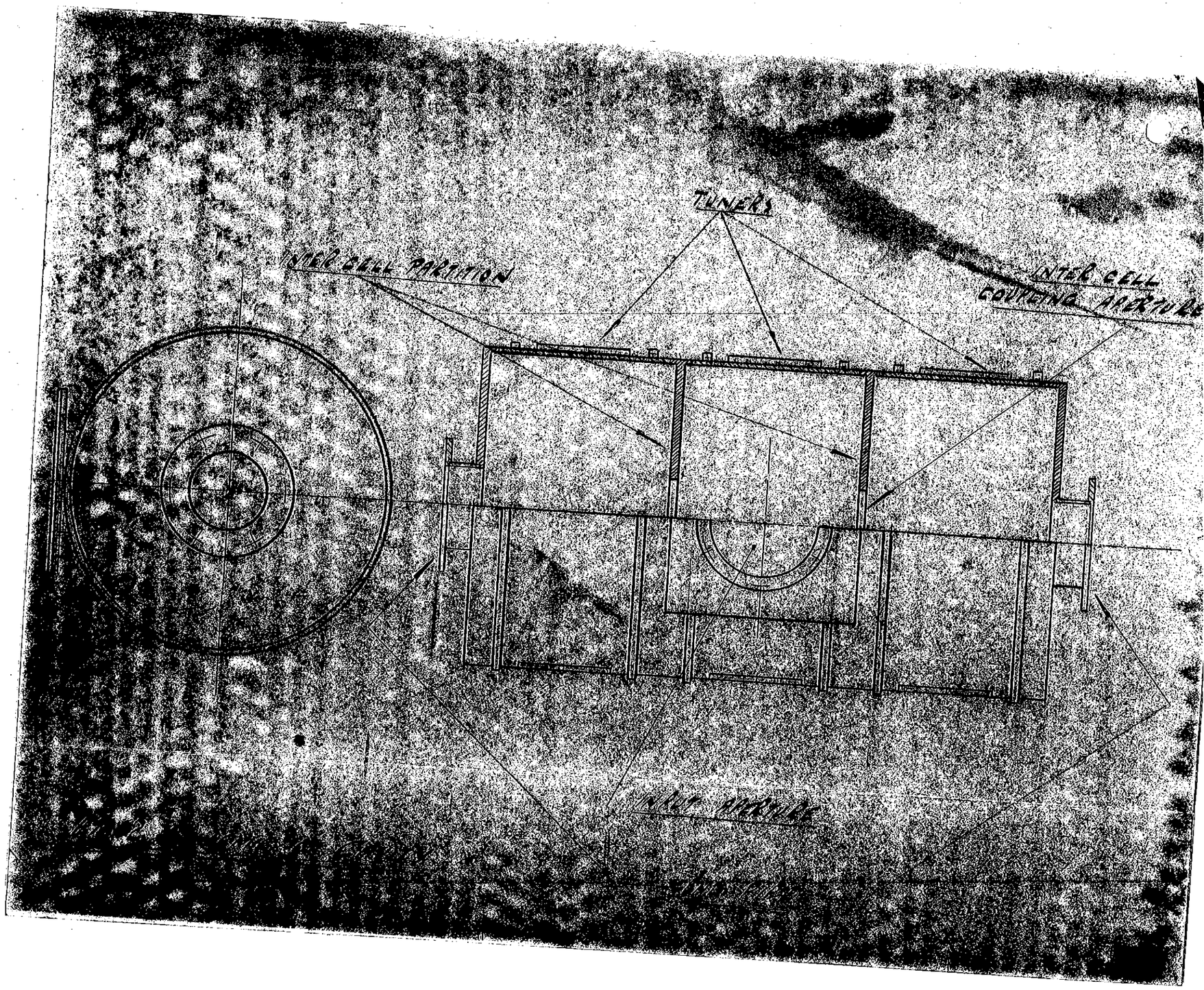
TUNERS
INTER CELL PARTITION
INTER CELL
COUPLING APERTURE

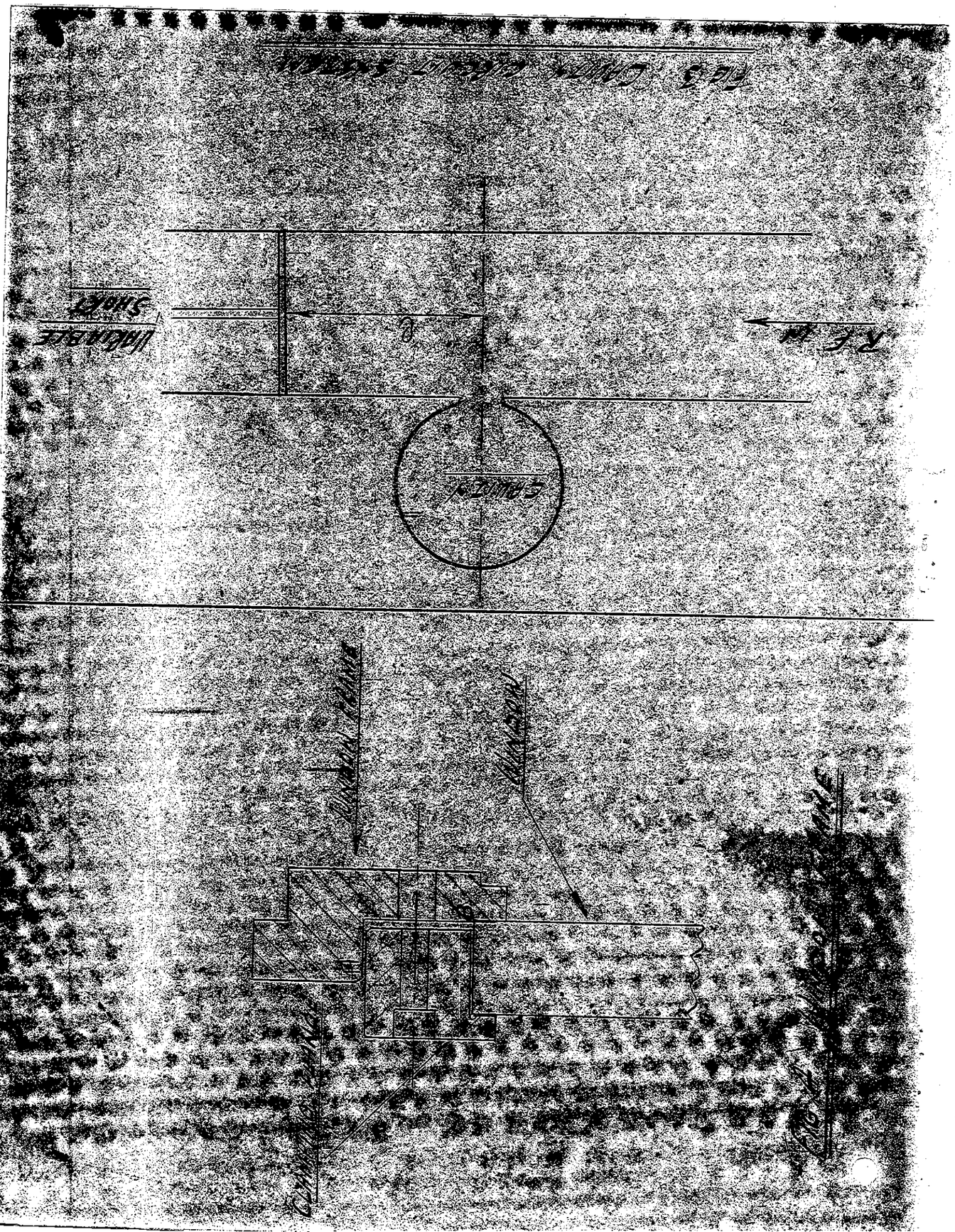

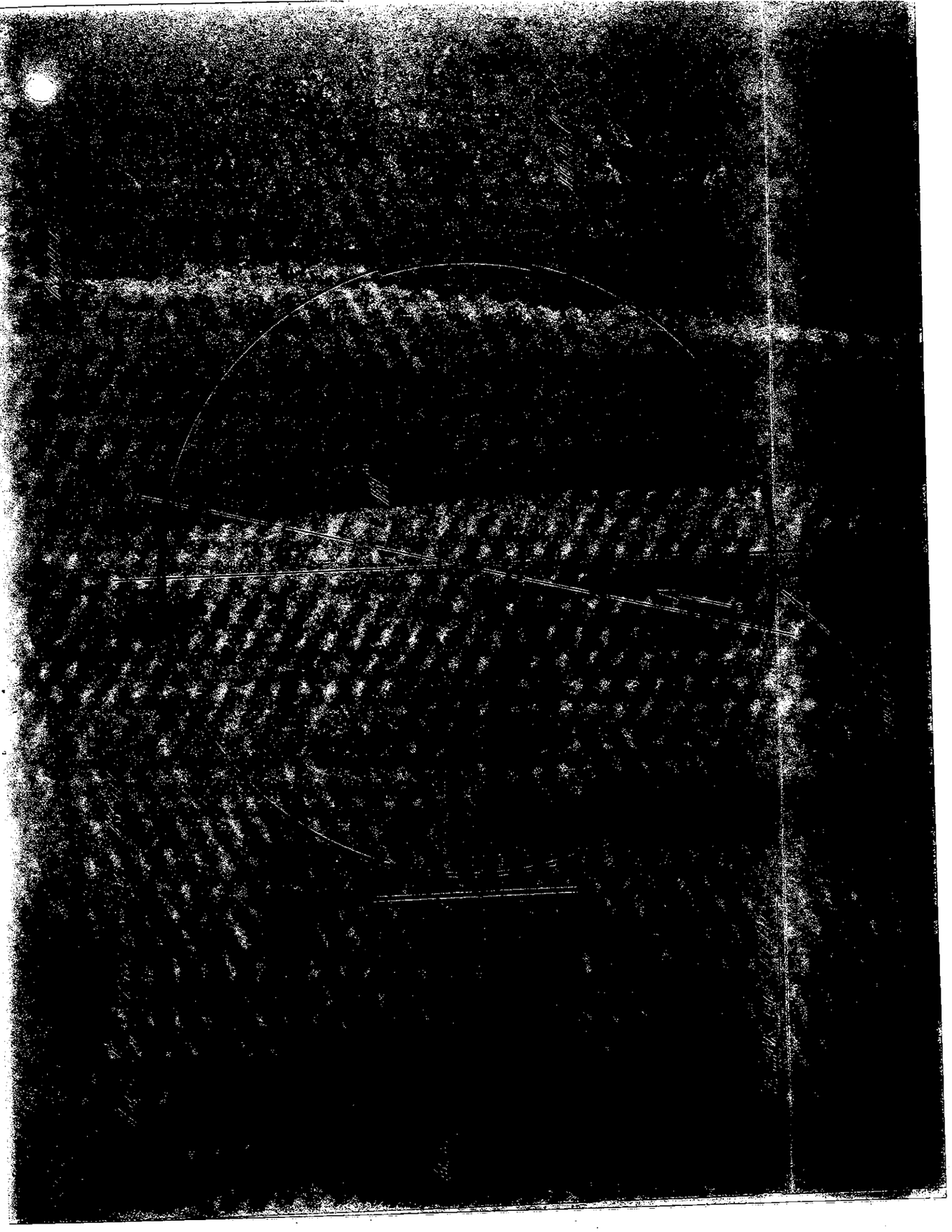

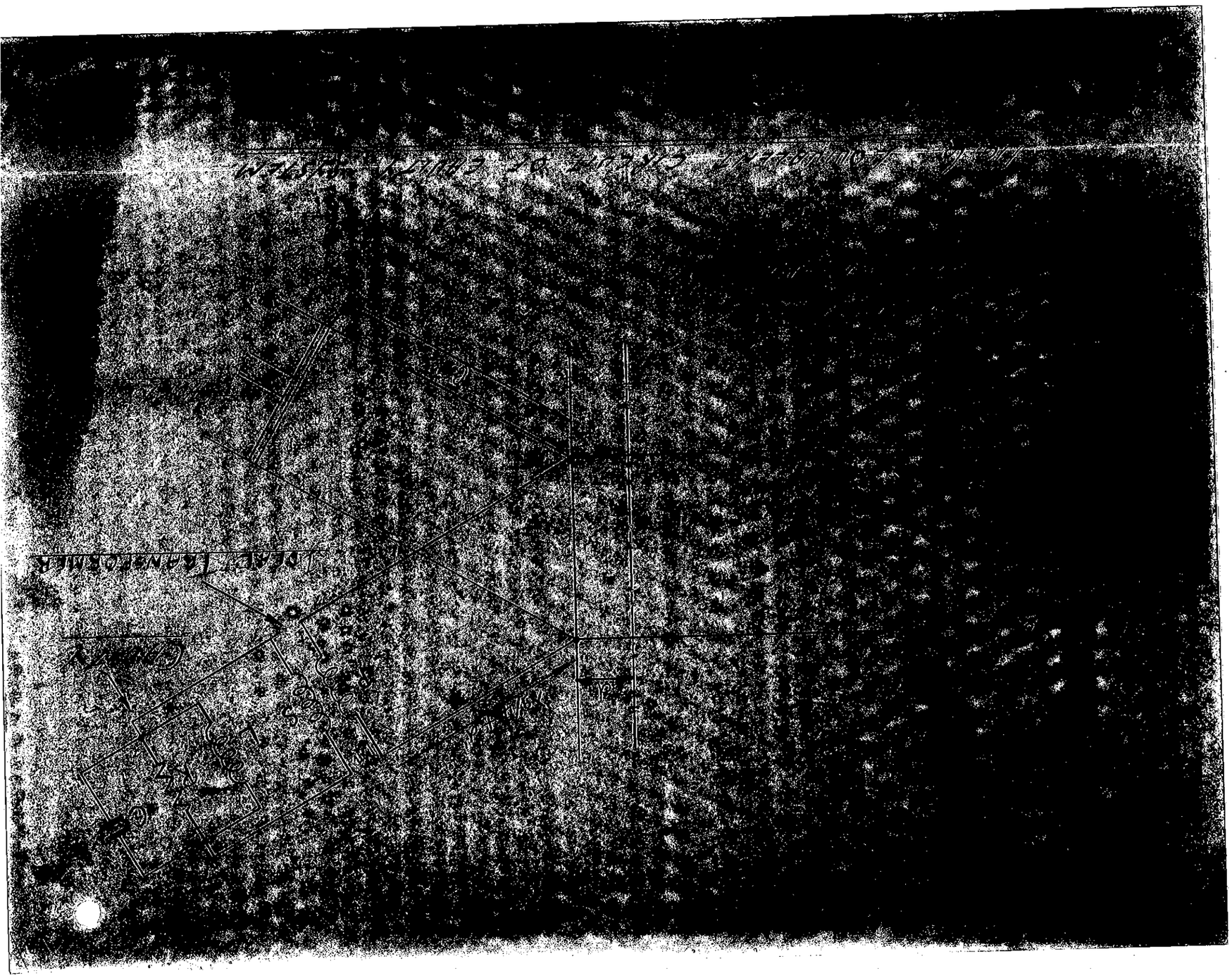
LAKE TAHOE

COUPLING FACTOR β vs. IRIS DIAMETER Ø : GRAPH No 1

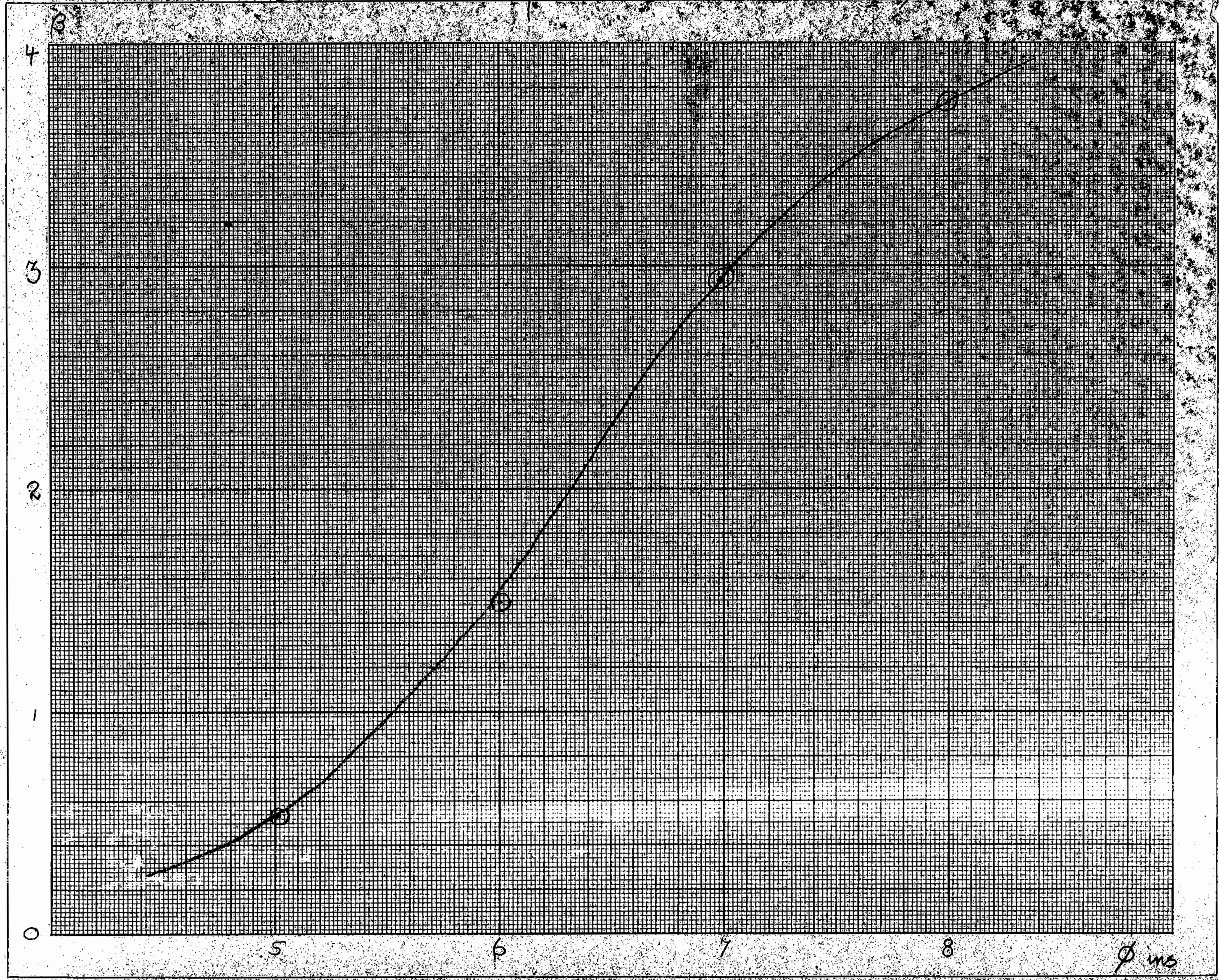

1/Q EXT V.S. IRIS DIAMETER Ø GRAPH Nº 2

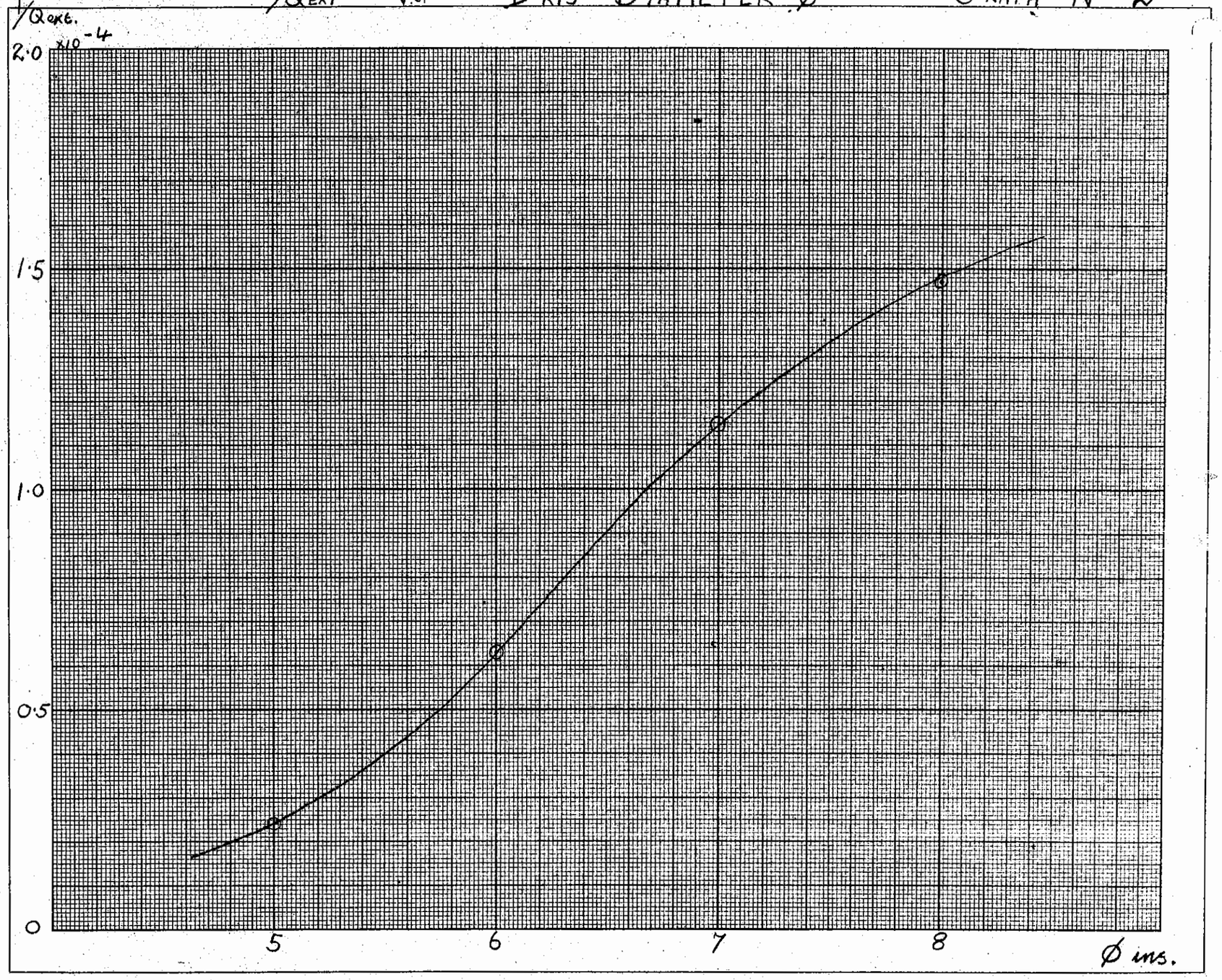

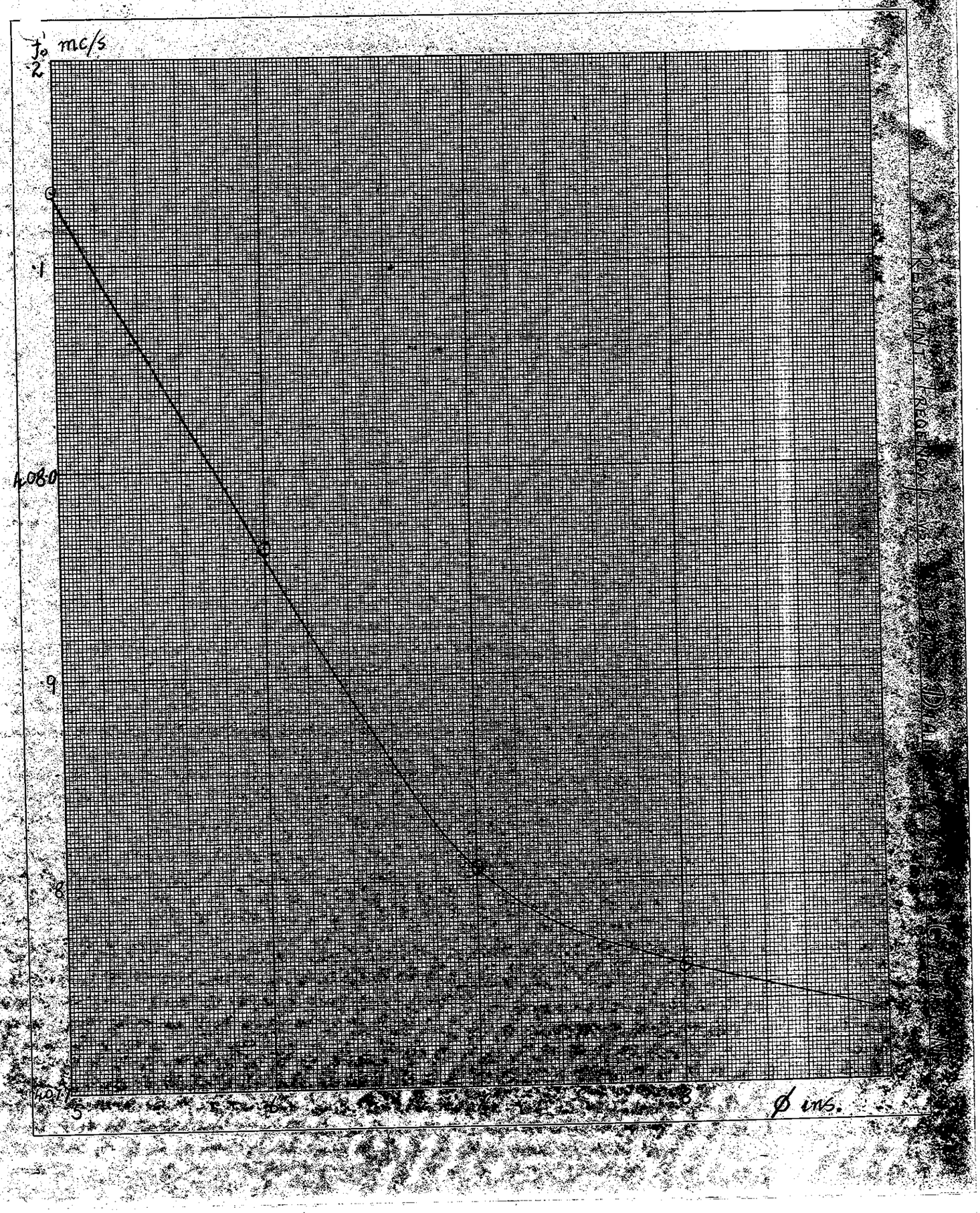
f_o mc/s
2
1
9
8
7
6
5
4080
RESONANT FREQUENCY VS
Ø ins.

PERTURBATION OF CAVITY BY METAL BEAD. GRAPH Nº 4

(AIR FILLED INPUT APERTURE)

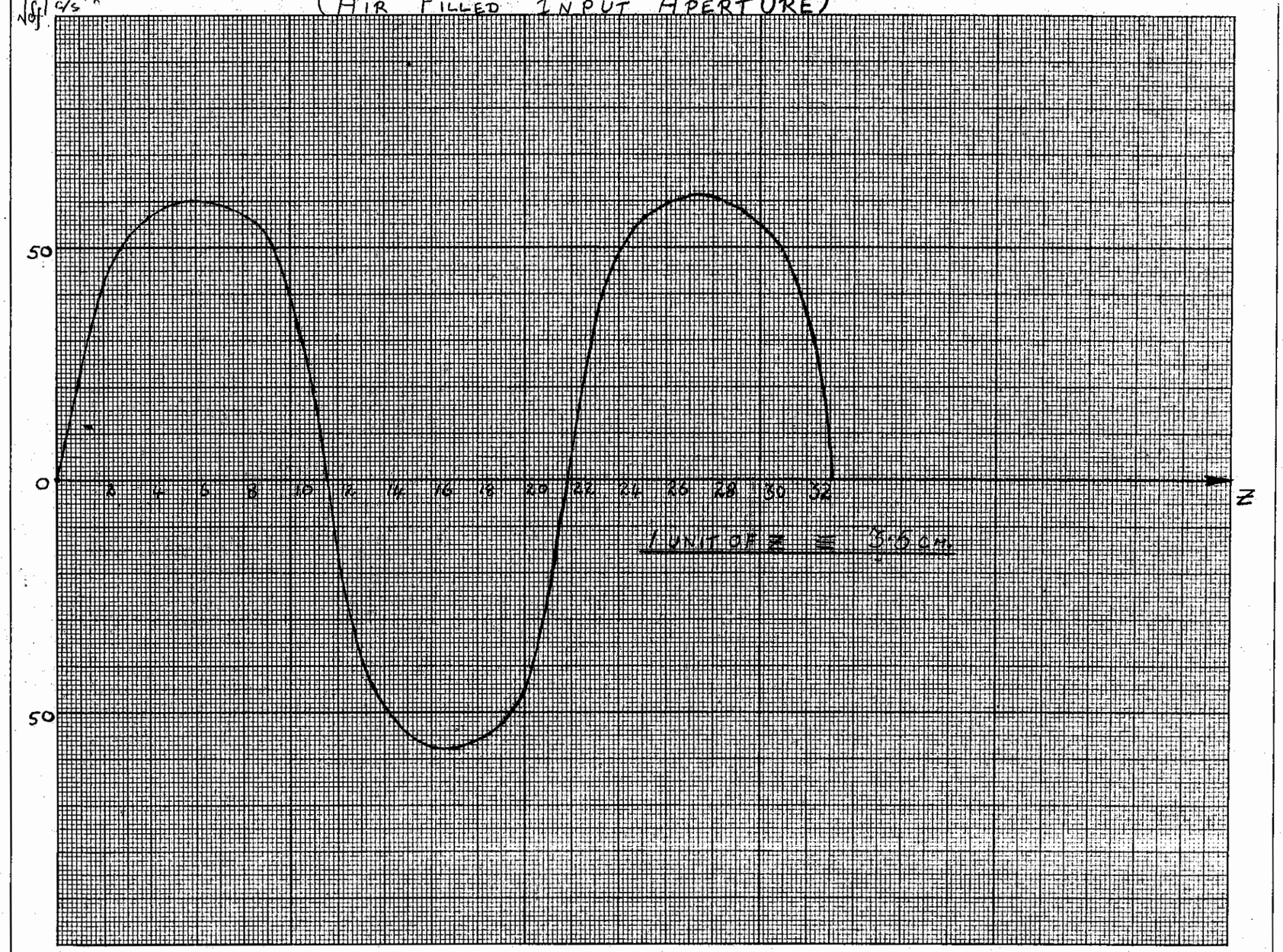

PERTURBATION OF CAVITY BY METAL BEAD (INPUT APERTURE 9/16" THICK ALUMINA) GRAPH Nº 5

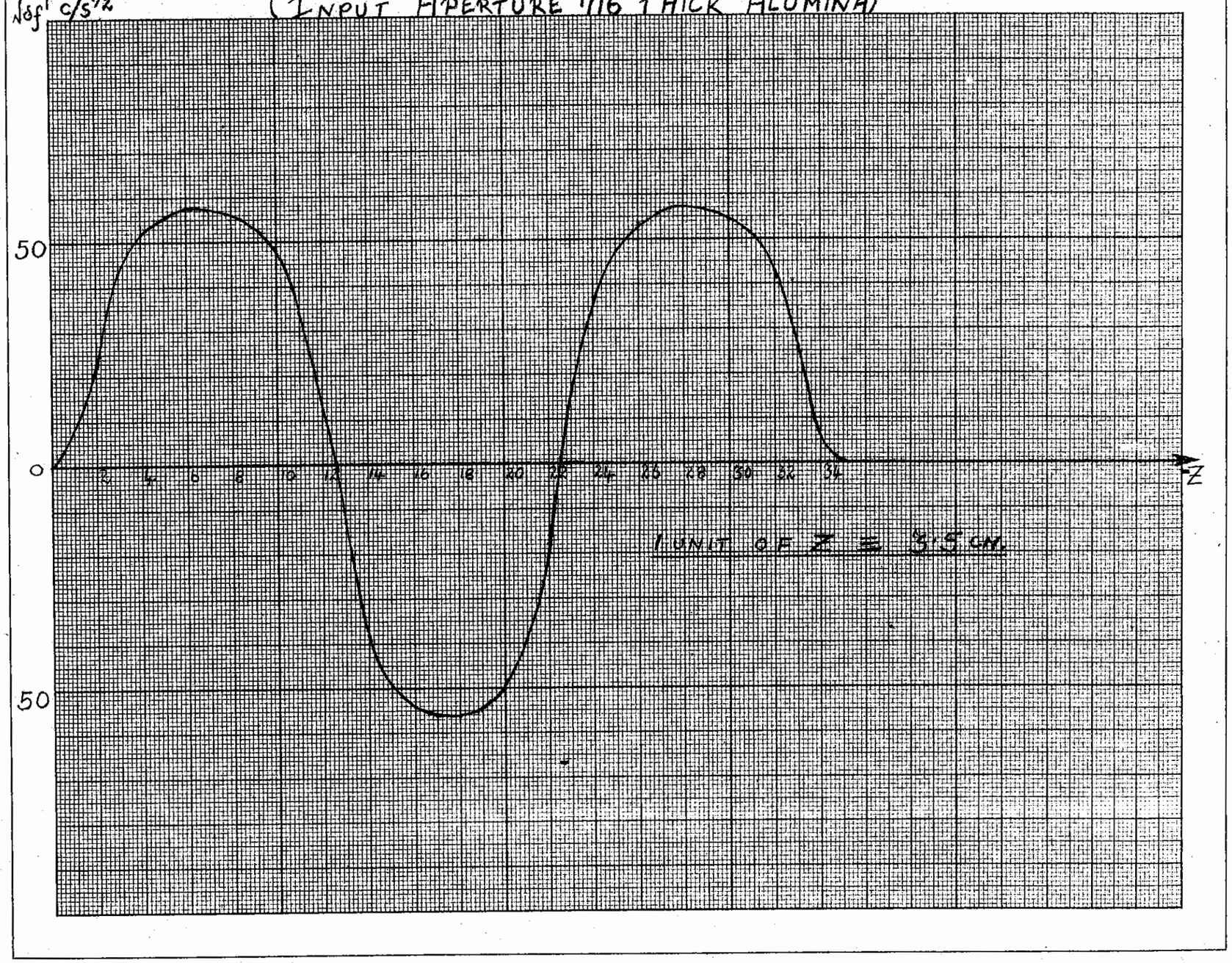

COMPARISON OF PERTURBATIONS DUE TO METAL & DIELECTRIC BEADS GRAPH No 6

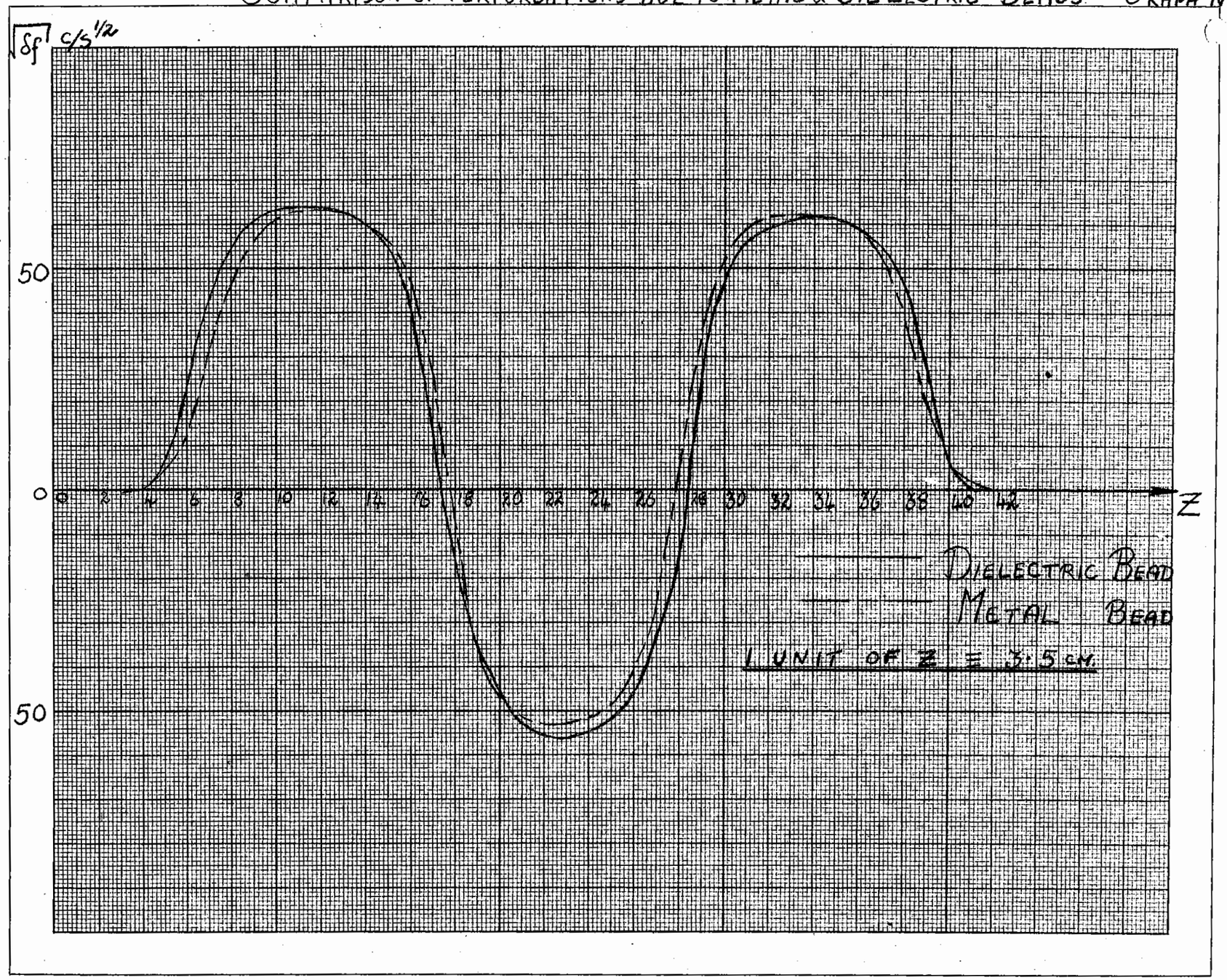

PERTURBATION OF CAVITY IN "O" MODE. GRAPH Nº 7

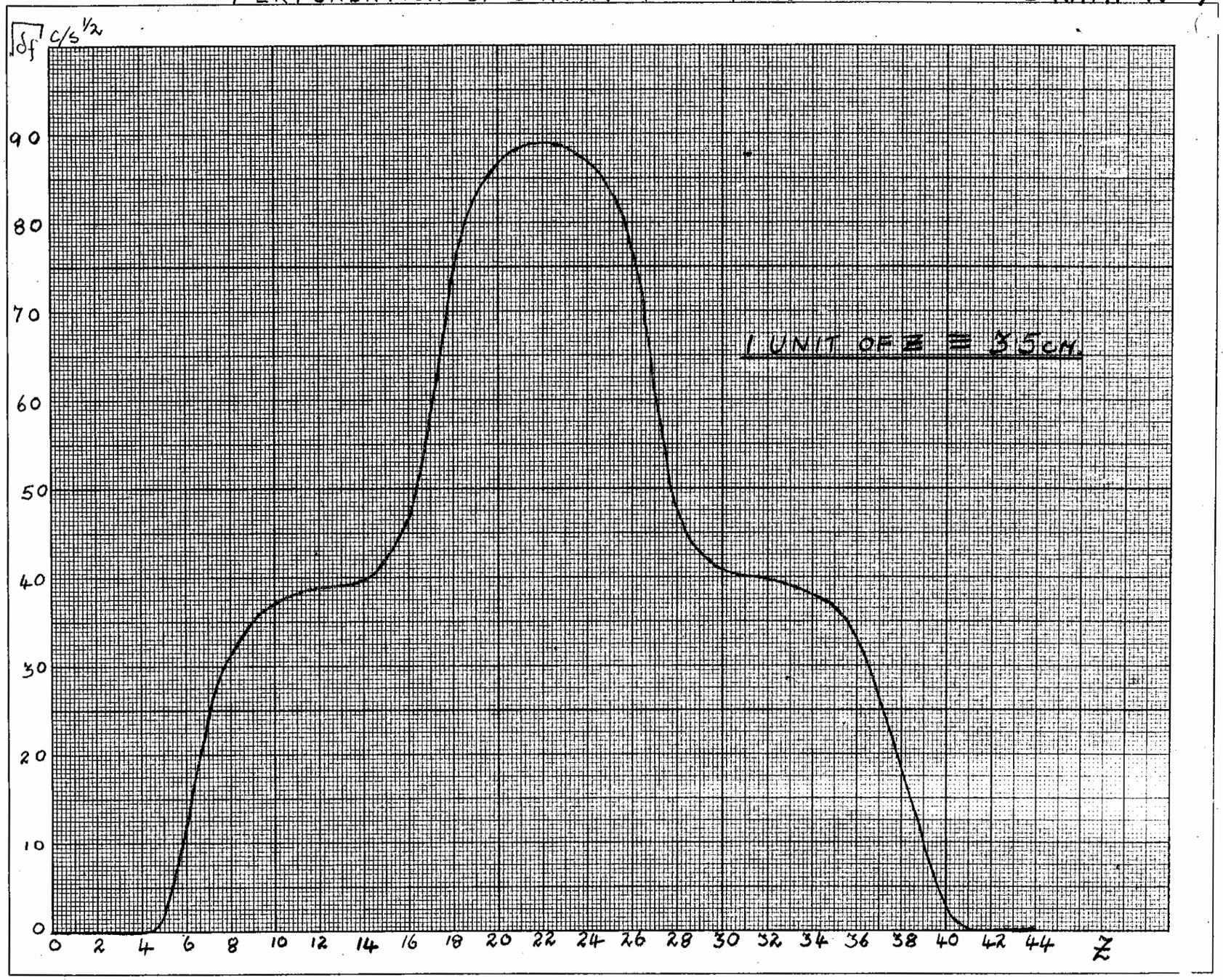

Effect of End Pipes.

Graph Nº 8

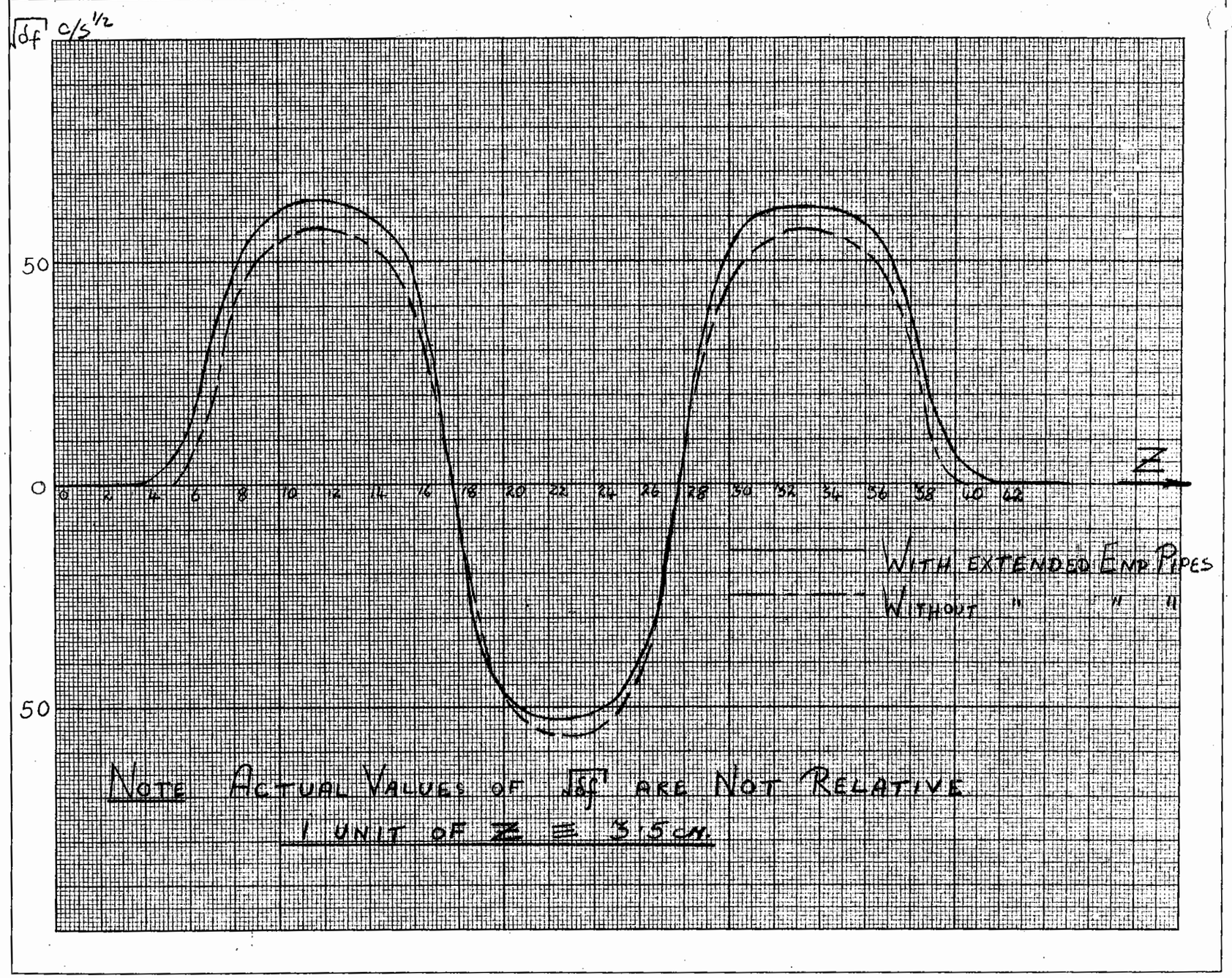

Note Actual Values of $\sqrt{df}$ are not Relative.

1 unit of Z = 3.5 cm.

RADIAL PERTURBATION OF CAVITY FIELDS

GRAPH Nº 9

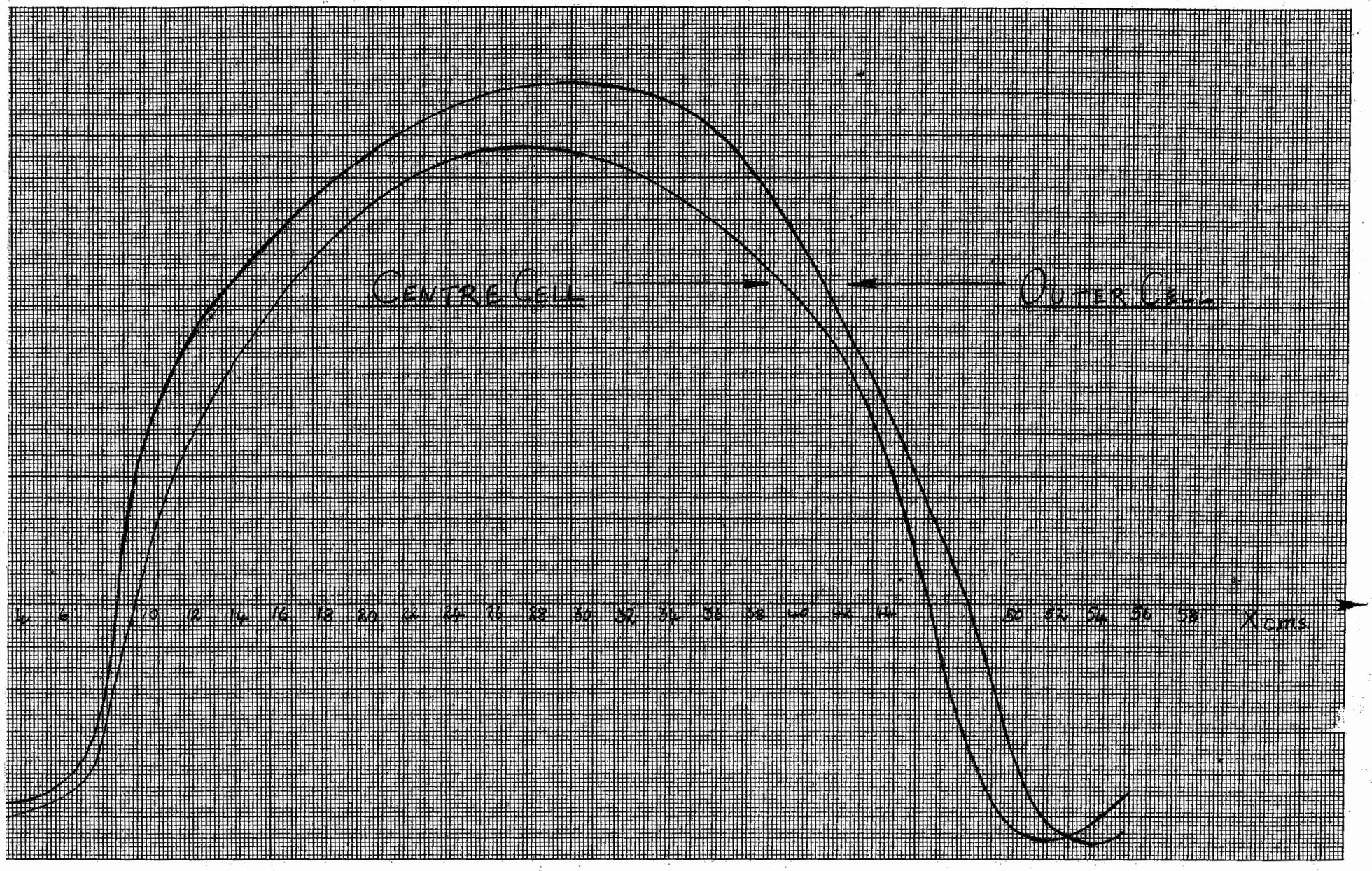

PERTURBATION OF LOADED CAVITY. GRAPH Nº 10

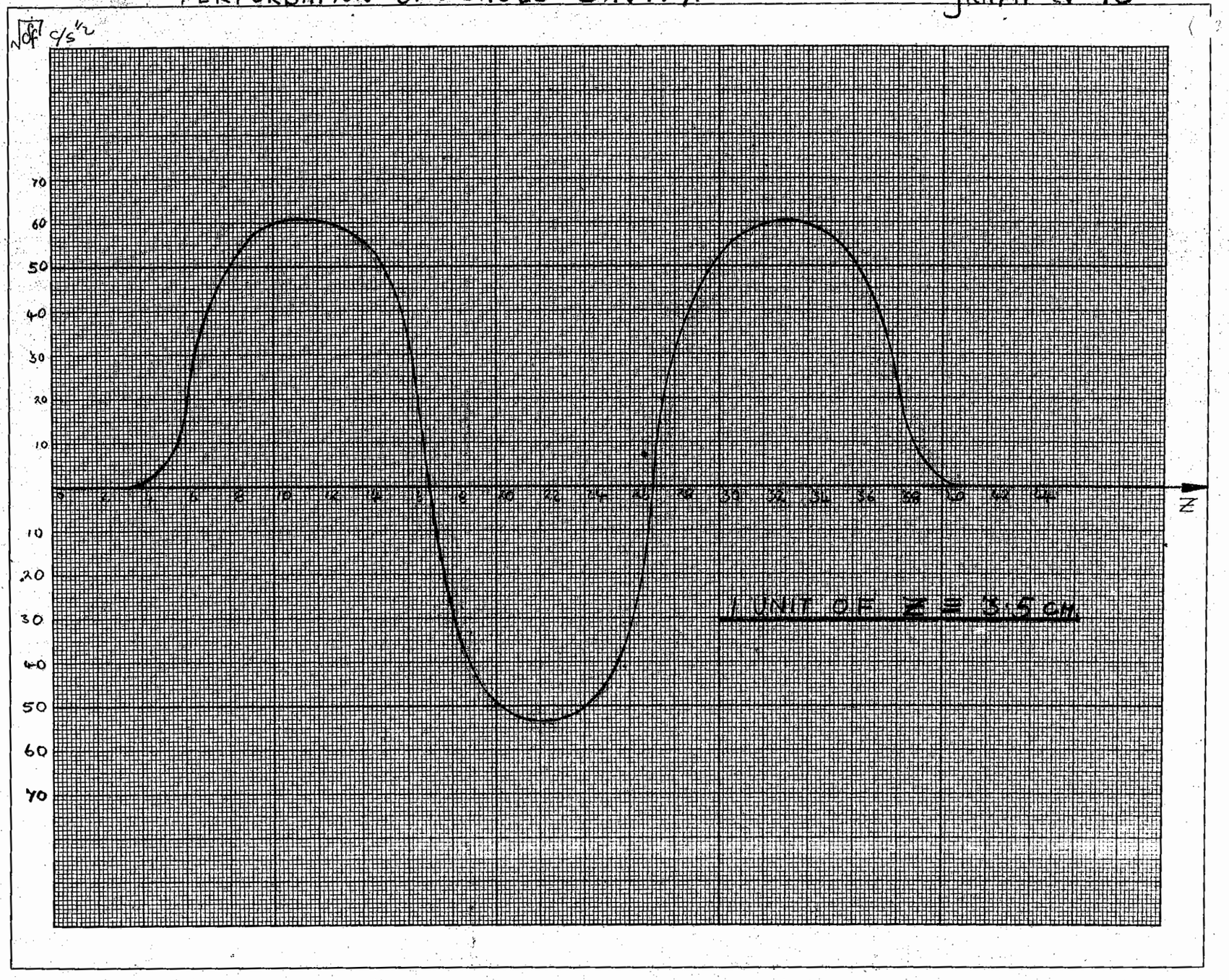

GRAPH SHEET No. 7510

IMPEDANCE CHART "A"

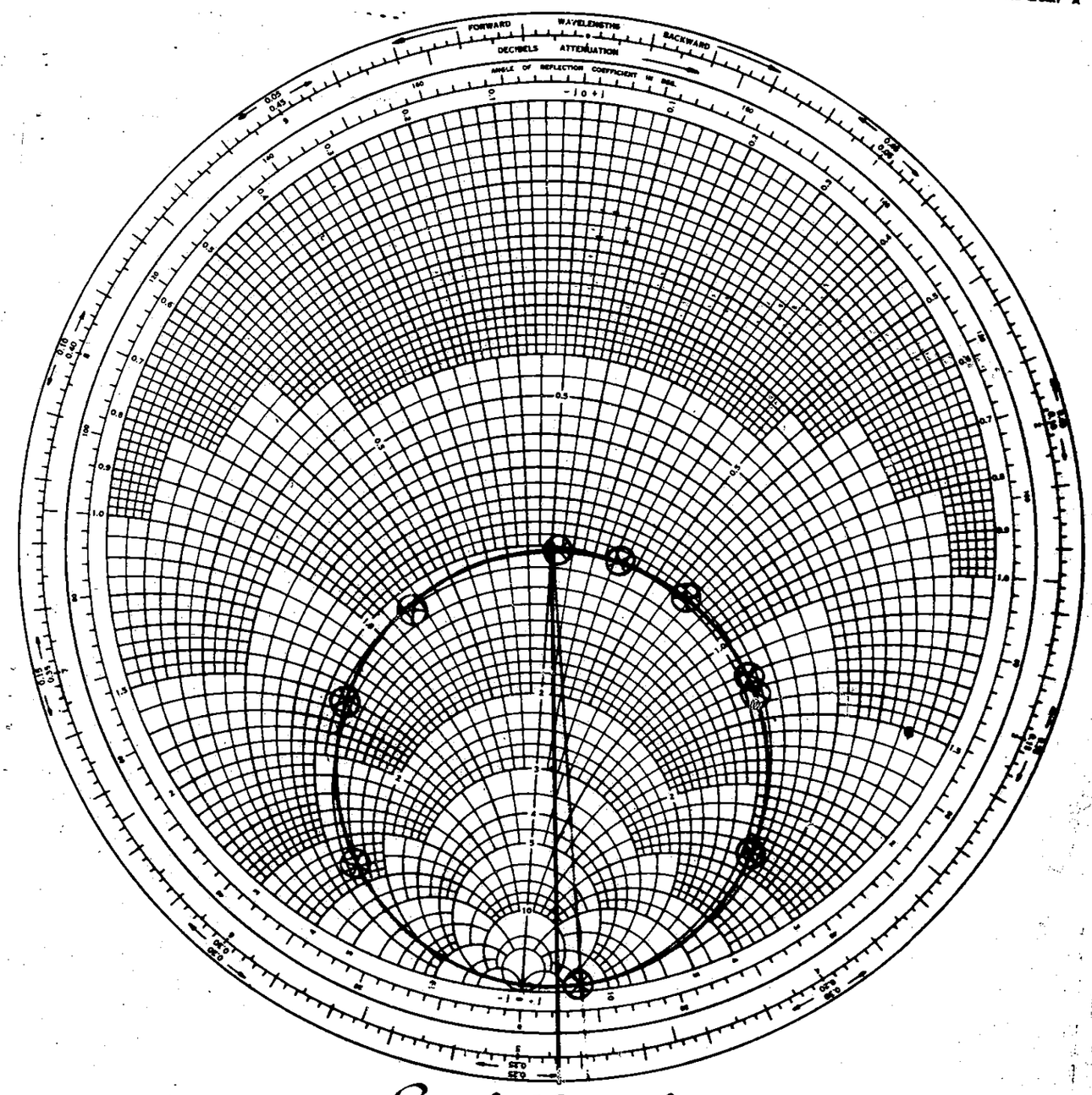

Smith Chart No 1

GRAPH SHEET No. 7510

IMPEDANCE CHART "R"

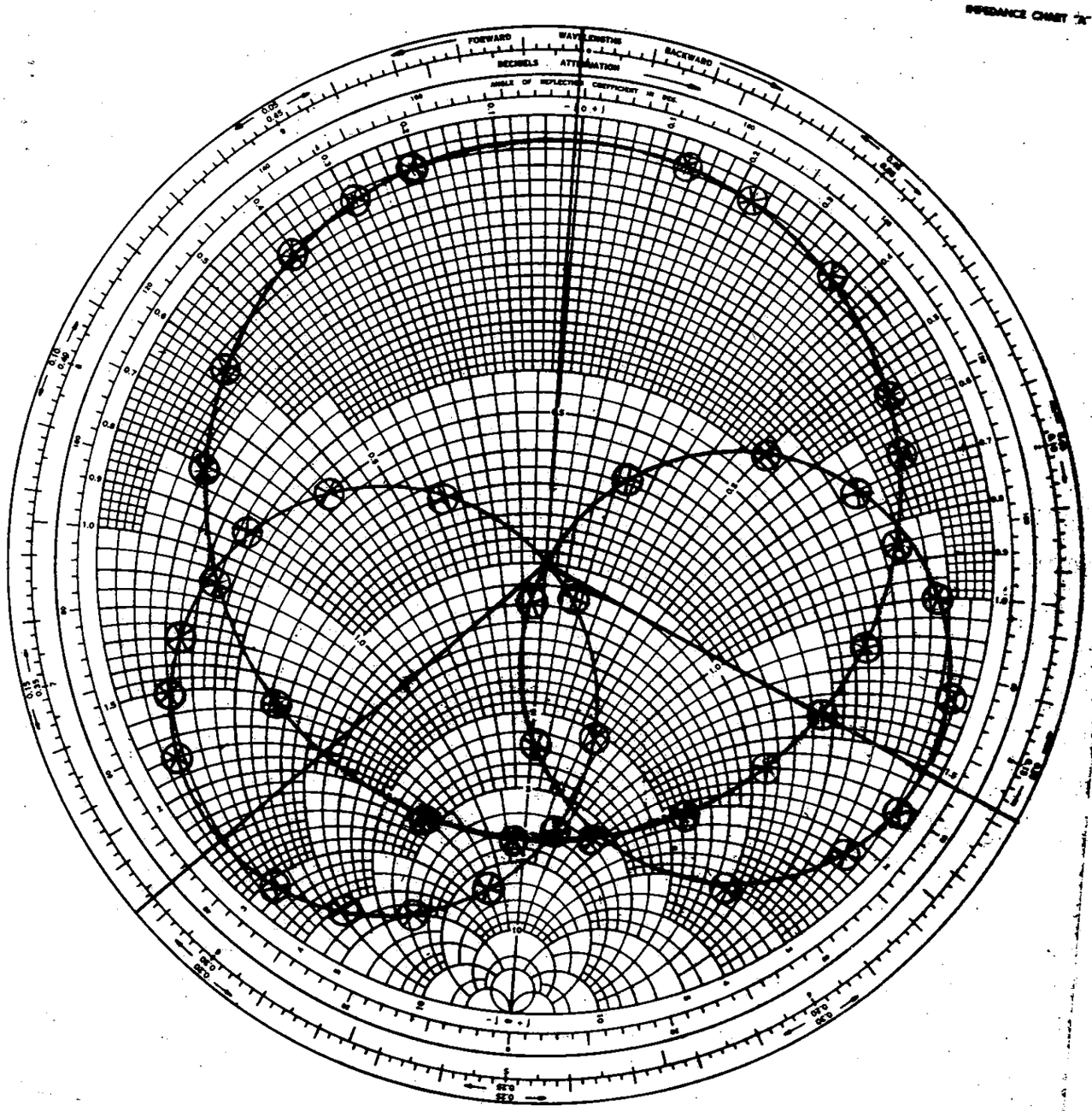

Smith Chart No 2

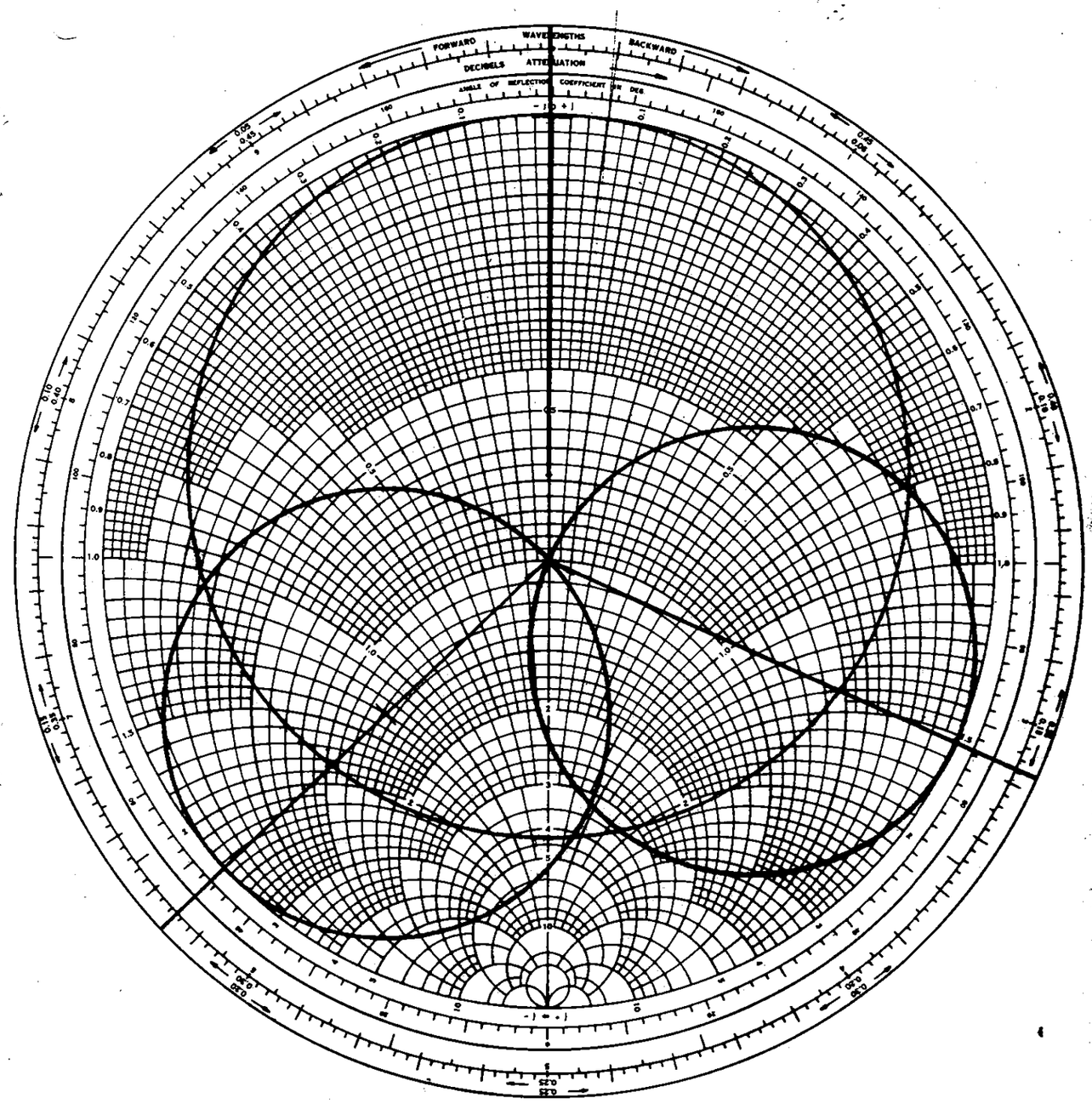

Smith Chart No 3

GRAPH SHEET No. 7510

IMPEDANCE CHART "A"

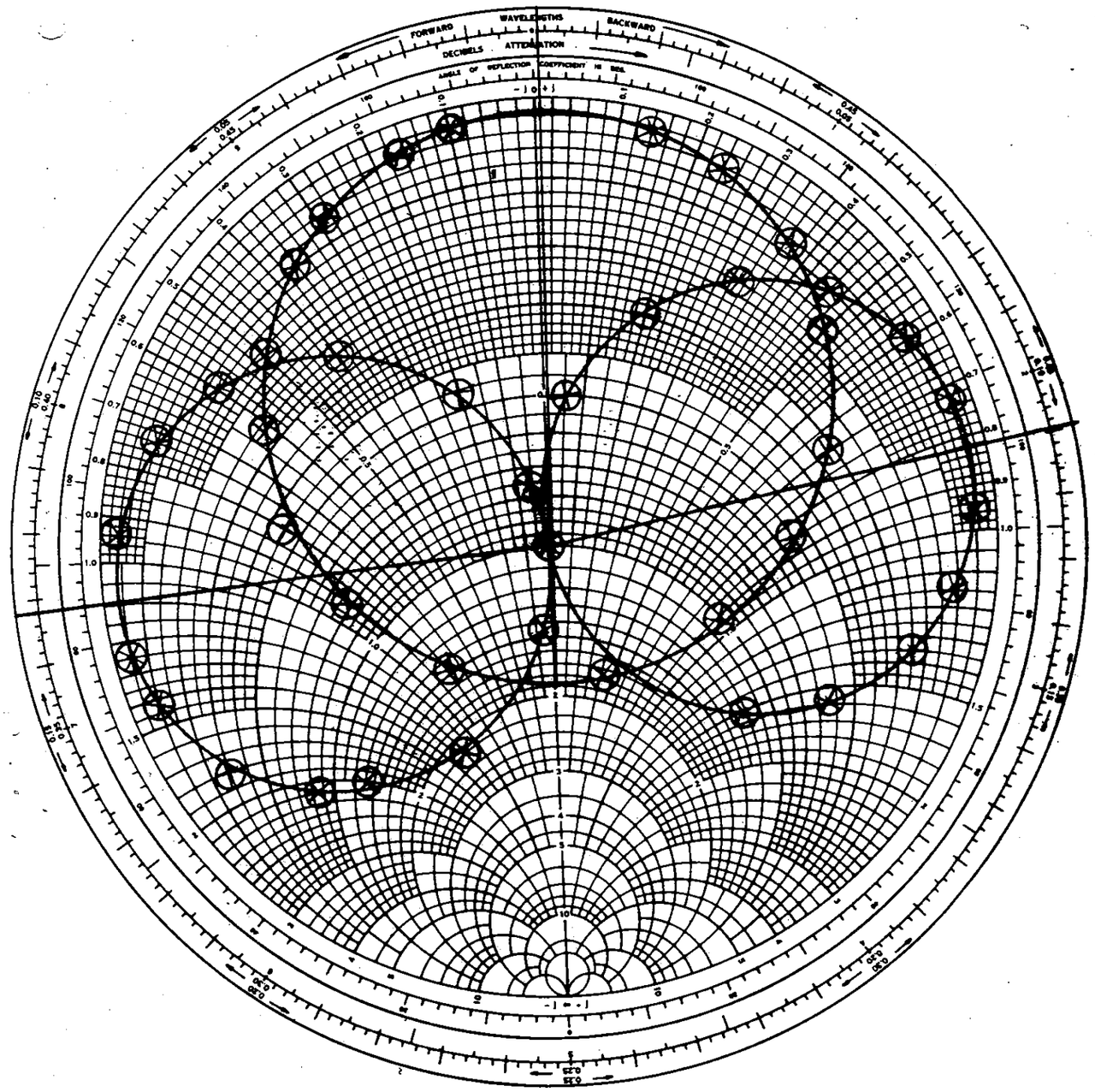

Smith Chart No 4

GRAPH SHEET No. 7510

IMPEDANCE CHART "A"

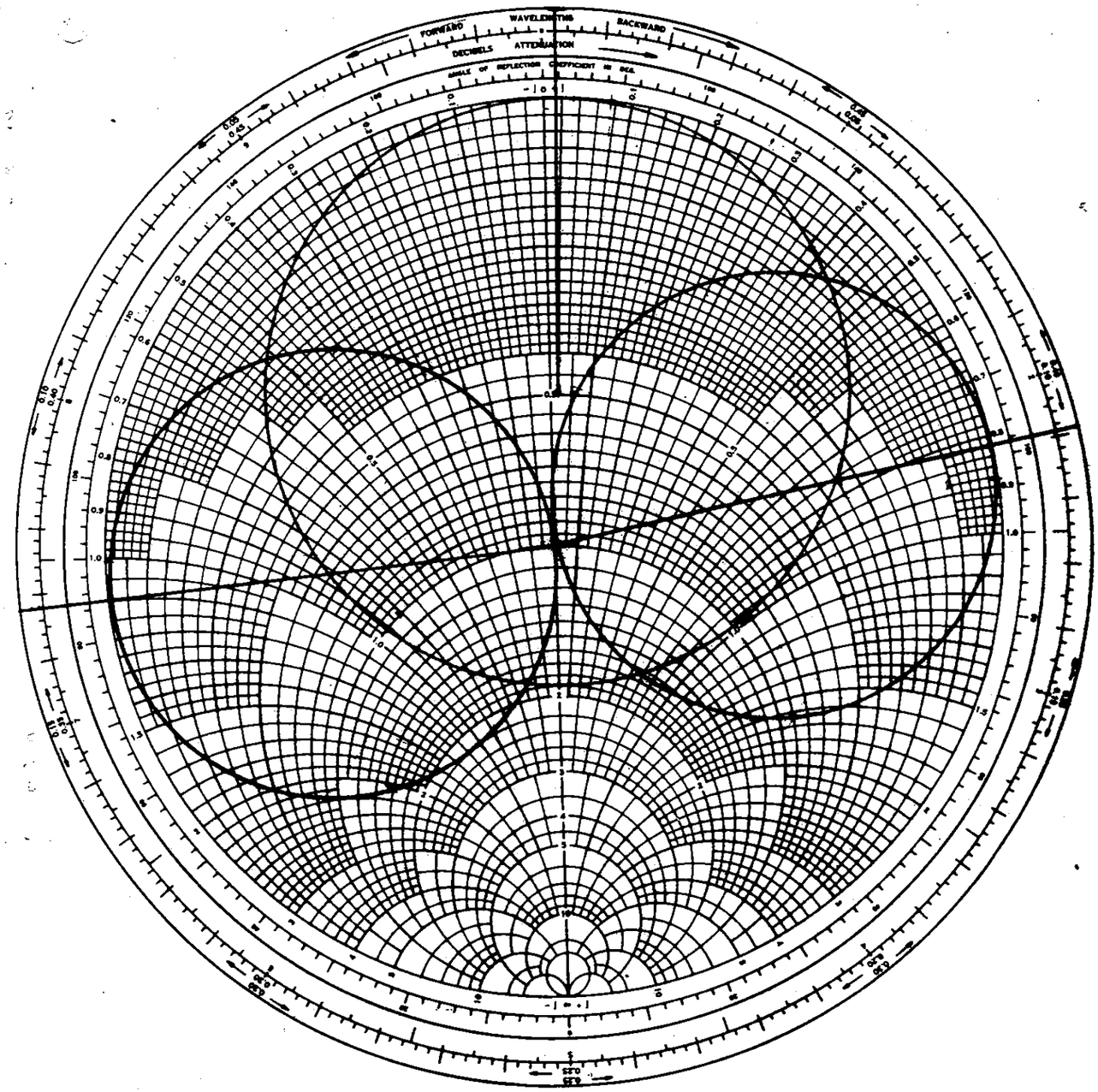

Smith Chart No.